revised: 6 Feb 2019 trf abg jwb

Report to DRBC on concentrations of nutrients and chlorophyll a and rates of respiration and primary production in samples from the Delaware River collected in May and July 2018

Thomas R. Fisher
Professor

Anne B. Gustafson
Senior Faculty Research Assistant

Horn Point Laboratory
Center for Environmental Science
University of Maryland
2020 Horn Point Road
Cambridge MD 21613

Introduction

In December 2012, the Delaware River Basin Commission (DRBC) convened a Modeling Expert Panel to initiate work on development of an eutrophication model of the Delaware Estuary. This model was envisioned as a needed step toward the development of updated water quality criteria for dissolved oxygen and numeric nutrient criteria for the estuary, as described in DRBC's Nutrient Criteria Development Plan (http://www.nj.gov/drbc/library/documents/nutrients/del-river-estuary_nutrient-plan_dec2013.pdf). The Expert Panel reviewed existing information with DRBC and recommended among other activities the collection of new primary productivity and respiration data in the Delaware River and Estuary. In 2014 we measured nutrients, oxygen, water column extinction coefficients, respiration, and primary productivity in the lower Delaware estuary (RM 0 – 40) as an initial response to the Expert Panel recommendation (Fisher and Gustafson 2015). In the current report we provide a similar set of data for the Delaware River (RM 71-131). In the Discussion section we make some comparisons between the two sets of data from the upper and lower sections of the Delaware Estuary.

As in 2014, sampling was conducted on two dates in 2018. On May 8, 2018 and July 9, 2018, DRBC staff collected surface and bottom water samples along five lateral transects at River Miles 71, 86, 101, 116, and 131. Samples were collected at three sites on each lateral transect (main channel, left of channel, and right of channel). At transects where the main channel ran along the shoreline, samples were collected at only two sites. A total of 13 sites were sampled, and 26 water samples were collected (see Table 1, Fig. 1). At each of the 13 sites, surface and bottom measurements of salinity, temperature, and dissolved oxygen (DO) were made, and DRBC also measured photosynthetically active radiation (PAR) above the water and at one meter below the water surface to provide data to estimate the PAR extinction coefficient (k, m^{-1}, see Methods below).

Methods

Field data were collected by DRBC personnel *in situ*. Salinity, temperature, and dissolved oxygen (DO) data at the surface and bottom were obtained using a Measurement Specialties Eureka 3 water quality meter. Light extinction measurements were made using a LiCor LI-1400 data logger connected to a LI-190 surface PAR sensor and a LI-192 underwater sensor. Both sensors had been recently calibrated by LiCor on January 19, 2018. At each station, surface irradiance (I_O, µE m^{-2} s^{-1}) was measured simultaneously with irradiance at a depth z = 1 m (I_Z, µE m^{-2} s^{-1}). The light extinction coefficient in the water column (k, m^{-1}) was estimated from these data as follows:

$$k = \ln(I_O/I_Z)/z = \ln(I_O/I_Z) \qquad \text{eq. 1}$$

for z = 1 m. These measurements were made *in situ* on the vessel when the water samples were taken for subsequent analysis of nutrients, respiration, and primary production in our laboratory.

Water samples were collected at 13 stations (13 surface samples, 13 bottom samples) as described in the introduction by DRBC personnel on an 18-foot jon boat . Collected water samples were maintained at ambient bay water temperature at 60% light (surface samples) or in darkness (bottom water samples) while on the ship. At the dock the samples were transferred late in the day to coolers to maintain river water temperature as much as possible, and the samples were then driven to HPL on the day of sampling. Within 1.5 h of the ship's arrival at the dock, the samples were transferred to a BOD box at the Horn Point Laboratory (HPL) maintained at 16.3°C in May and 25.7°C in July to approximate the median bay temperatures observed (range = 16.1-18.0°C in May, 25.5-27.0°C in July). Lights within the box provided ~100 µE m^{-2} s^{-1} of PAR on the appropriate day/night cycle for the month. Bottom samples were wrapped in black bags within the BOD box to maintain darkness and ambient temperature. On the morning following sample collection, aliquots of the samples were placed in incubation bottles for measurements of respiration (all samples) and ^{14}C-based primary production (surface samples only). Details are provided below.

Samples for nutrient (NH_4, NO_2+NO_3, and PO_4, µM = µmoles L^{-1} = mmoles m^{-3}) and chlorophyll a (chla, µg L^{-1} = mg m^{-3}) analyses were filtered following the start of the incubations. Filtered samples were frozen at -5°C and analyzed for nutrients within two weeks by automated colorimetry on a Technicon 2 AutoAnalyzer in the HPL Analytical Services Laboratory following the protocols of Lane et al (2000). The protocols followed EPA standard methods 350.1 for NH_4, 353.2 for NO_3 + NO_2, and 365.1 for PO_4 (soluble reactive phosphate). Filters for chla analysis were frozen and stored at -80◦C until analysis by fluorometry on a Turner Designs model 10-AU in the HPL Analytical Services Laboratory, generally within 2 months. The chla protocol followed the EPA 445.0 standard method.

Respiration was measured as the difference in oxygen concentrations (O_2, mg O_2 L^{-1}) between an initial measurement and a final measurement after a dark incubation of ~24 hours. Initial and final samples were put into quadruplicate, 12 ml, darkened, Exetainer tubes with septa caps (Labco, Inc.) to exclude air contact. The initial samples were processed in sequence within two hours as described below, and the remaining bottles were transferred to an incubator floating in the HPL boat basin subject to Choptank River temperatures and weak wave action. Final samples were returned to the lab ~24 hours later and were also analyzed in sequence for O_2 on the same day. All of the respiration samples were analyzed for O_2 by Membrane Inlet Mass Spectrometry (MIMS, Kana et al. 1994) with a precision of <0.5%. The first replicate of each set of four for each sample was used to condition the MIMS, and the remaining three were averaged for DO. MIMS simultaneously measures dissolved N_2, O_2, and Ar with high precision, and the ratios of N_2 and O_2 to Ar can be used to assess saturation relative to air equilibrium. The difference between the initial and final DO (DO_i, DO_f, mg O_2 L^{-1}) was used to calculate Respiration (R, mg O_2 L^{-1} d^{-1}, equivalent to g O_2 m^{-3} d^{-1}), as follows:

$$R = (DO_f - DO_i)/\Delta t \qquad \text{eq. 2}$$

where Δt = time in days calculated from the average time of initial and final analyses for each station. Since DO_i was always greater than DO_f, with one exception, R was always negative, representing

consumption of O_2. For the one exception at station RM-86-RS top, there was an anomalous increase in O_2, and we have not used the respiration value from this surface station in the analyses below.

Primary production measurements were performed on the samples stored overnight in the BOD box maintained at an appropriate diel light regime (described above). Six aliquots of sample (148 ml) were transferred to rinsed, transparent, 150 ml bottles. We added 0.1 ml of a ^{14}C-$NaHCO_3$ solution (1 µCi/ml activity) to each bottle, capped each bottle, mixed thoroughly, and filtered one of the bottles immediately to correct for particulate contaminants in the stock and ^{14}C sorption on particulates in the original water sample. The other five bottles were transferred into screened bags of varying thicknesses to attenuate the light to 60%, 32%, 15%, 7.5%, and 3.0% of surface Photosynthetically Active Radiation (PAR, 400-700 nm, E m^{-2} d^{-1}), which was monitored on the roof of HPL and calculated as described in Fisher et al. (2003). The bottles in their screens were then quickly transferred to the floating incubator described above, and incubated for ~24 hours, when they were returned to the laboratory for filtration. Following filtration on 25 mm GFF filters at <200 mm Hg vacuum, all filters (including the edges under the filter funnel) were rinsed with filtered sample water from the original sample to remove dissolved ^{14}C and then transferred to 7 ml scintillation vials with 7 ml of Ecoscint A fluor. Total ^{14}C activity (TA, dpm/ml) was measured using the addition of 0.1 ml of the ^{14}C stock to Ecoscint A fluor. All scintillation vials were allowed to sit for 24 hours in the Packard Tricarb model 2200CA liquid scintillation counter to eliminate auto-fluorescence from ambient light, and then counted to 1% counting accuracy. Total CO_2 (TCO_2 = sum of CO_2, H_2CO_3, HCO_3^-, and CO_3^{-2}) was calculated using the relationship of carbonate alkalinity to salinity reported for Delaware Bay by Sharp (2013). Primary production at simulated depth z (P_Z, mg C L^{-1} d^{-1} = g C m^{-3} d^{-1}) was calculated as follows:

$$P_Z = 1.05 * TCO_2 * (DPM_f - DPM_i) / (TA * \Delta t) \qquad \text{eq. 3}$$

where 1.05 corrects for the isotopic discrimination for ^{14}C-CO_2 uptake compared to ^{12}C-CO_2 uptake, DPM_f and DPM_i are the ^{14}C activity of the final and initial samples for each light level, and Δt is the time

interval in days (approximately 1 day).

In general, we adhered to the protocols of Sharp et al. (2009) and Sharp (2013) for primary production measurements to maintain continuity with existing primary production datasets. Deviations from Sharp's protocols included: (1) lower ^{14}C activity added to our samples (0.1 μCi in 150 ml bottles vs 1 μCi in 80 ml bottles by Sharp), and (2) our attenuation screens were virtually identical to those used by Sharp, but we used a 3% compared to a 1.5% PAR level for the highest light attenuation (lowest light level). Neither of these deviations should have any significant effect on the rates of primary production at a given depth (P_Z, g C m^{-3} d^{-1}) or integrated primary productivity (P, g C m^{-2} d^{-1}) reported here for comparison with Sharp's previous datasets.

We used the hyperbolic tangent model of Jassby and Platt (1976) to evaluate the effect of PAR on rates of primary production at any depth z (m) as (P_Z):

$$P_Z = P_m * \tanh(x) \qquad \text{eq. 4}$$

where P_m is the maximum, light-saturated primary production (g C m^{-3} d^{-1}). P_m is the asymptote as P_Z approaches saturation, and x is a composite parameter defined as follows:

$$x = \alpha * PAR / P_m \qquad \text{eq. 5}$$

where α is the light-dependent primary productivity parameter (initial slope of P_Z vs PAR with units of g C m^{-3} (E m^{-2})$^{-1}$. Values of P_Z for each station at varying PAR were fit with the hyperbolic tangent function to obtain α and P_m. This equation is equivalent to models 1 (linear) and 2 (hyperbolic saturation) used by Sharp (2013). In the dataset reported for May and July 2014 in Delaware Bay (Fisher and Gustafson 2015) and for May and July 2018 in the Delaware River (this report), we saw no evidence of light inhibition (Sharp's model 3).

For ease of fitting the hyperbolic tangent (tanh) function to the P_Z vs PAR data in SigmaPlot v12.5, we used the following transformation:

$$\tanh(x) = (e^{2x} - 1)/(e^{2x} + 1) \qquad \text{eq. 6}$$

which was obtained from:

http://www.roperld.com/science/Mathematics/HyperbolicTangentWorld.htm

In our application, we used the following formulation:

$$P_Z = P_m * (e^{2*\alpha*PAR/Pm} -1)/(e^{2*\alpha*PAR/Pm} +1) \quad \text{eq.7}$$

where e is the exponential function, and all other parameters are described above. The hyperbolic tangent function fit the data well (r^2 generally > 0.90, see Fig. 2A, Tables 3A and 3B), and we were able to estimate α, the light-dependent primary production parameter (g C m^{-3} (E m^{-2})$^{-1}$) for every station. However, for eight of the May 2018 samples and three of the July 2018 samples, the relationship between P and PAR was essentially linear (Sharp's model 1), which enabled us to obtain α, but which prevented us from estimating P_m, the light-saturated primary production parameter (P_m, g C m^{-3} h^{-1}), which is independent of PAR. For consistency, we used eq. 7 to calculate α for all stations, but for eight May stations and three July stations, P_m was indeterminate.

We estimated integrated water column primary productivity (P, g C m^{-2} d^{-1}) using the measured water column extinction coefficient (k, m^{-1}, eq. 1) and the observed values of C fixation (P_Z) at the fixed light depths of 3-60%. Using k, we converted the light depth into water depth (z, m):

$$z = \ln(I_O/I_Z)/k \quad \text{eq. 8}$$

where I_O is the total PAR (E m^{-2} d^{-1}) during the incubations and I_Z is the calculated irradiance at the light depth (E m^{-2} d^{-1}) based on the station k. I_O was obtained using a LiCor- 190 surface probe on the roof of a building at Horn Point Laboratory attached to a LI-1000 data logger (see Fisher et al. 2003) integrated at hourly intervals (May: 42 E m^{-2} d^{-1}, July: 31 E m^{-2} d^{-1}). We extrapolated the observed volumetric C fixation rate at each depth to the midpoint between each depth above and below (Δz, m), except that the production at 60% light was extrapolated to the surface and the production at 3% light was extrapolated to one additional depth increment below the estimated value (see Fig. 6B). P was estimated as:

$$P = \Sigma (Pz * \Delta z) \qquad \text{eq. 9}$$

See Fig. 6B for an example.

All statistical analyses were done in SigmaPlot v12.5 and Excel 2010. The significance level for statistical tests was set at $p<0.05$ (significant) or $p<0.01$ (highly significant), unless otherwise noted. When terms with errors were combined in a formula, propagation of error for the final result was based on error in the individual components using the standard error propagation formulas in Bevington (1969), assuming no error covariance. Parametric statistical comparisons and tests were done if the data were normally distributed; otherwise an equivalent non-parametric test was used.

Results and Discussion

Nutrients

Concentrations of dissolved nutrients were generally high on both cruises in 2018 (Tables 1 and 2). Ammonium (NH_4^+) ranged over 0.6 – 24.1 µM on both cruises, averaging 10.1 ± 1.3 in May and significantly lower in July (1.3 ± 0.2, $p<0.05$). There were no significant differences ($p>0.10$) between surface and bottom water NH_4^+ at all stations on each cruise, although there was some lateral variability across the river for NH_4^+ and phosphate (PO_4^{-3}, Fig. 2). Nitrate (NO_3^-) was more abundant than ammonium, ranging over 46 - 166 µM on both cruises and averaging 67 ± 4 in May and significantly higher in July (114 ± 7, $p<0.05$). As for NH_4^+, there were no significant differences ($p>0.10$) in NO_3^- concentrations between surface and bottom waters at each station and little lateral variability. Phosphate had the lowest concentrations of the three major nutrients, ranging over 0.47- 2.05 µM on both cruises and averaging 0.70 ± 0.02 in May and significantly higher in July (1.80 ± 0.05, $p>0.05$). Comparing the seasonal differences in the two cruises, NO_3^- and PO_4^{-3} were both higher in the July cruise, and NH_4^+ was higher in May.

All of the concentrations reported in Tables 1 and 2 are considered saturating for phytoplankton growth in estuaries (Fisher et al. 1995, 1999). For all stations, both dissolved inorganic N (DIN = NO_3^- + NH_4^+) and PO_4^{-3} were sufficiently abundant that it is likely that light and not nutrients were limiting phytoplankton growth rates. As shown below, there was little evidence for vertical stratification, and deep mixing occurred in these upper Delaware River stations with moderate to high turbidity.

In our 2014 report on the lower Delaware Bay, we explored nutrient concentrations across the salinity gradient to illustrate net ecosystem processing. However, we are unable to explore the mixing behavior of nutrients in this report because all of the stations were fresh. Salinities ranged over 0.1-0.3 in both May and July, with <0.003 salinity differences between top and bottom samples. Temperatures ranged over 16-18°C in May and 25-28°C in July, with <0.3°C temperature differences between top and

bottom samples (Tables 1 and 2). Therefore, there was no evidence of significant surface to bottom differences in density or stratification at any of the stations.

To show the longitudinal distributions of nutrients, we have plotted them as a function of river mile (RM, Fig. 2). For both cruises, the spatial distribution of NO_3^- between RM 70 to 131 (top panel) exhibited a maximum at RM 71-86 near Wilmington DE, decreasing upstream towards Trenton. The systematically lower NO_3^- in May compared to July is also clearly shown. Ammonium in May had a spatial distribution with a maximum concentration of 16-24 µM at RM86 near the NO_3^- maximum. In contrast, NH_4^+ in July was low 1-4 µM, declining steadily downstream from Trenton to Wilmington. Although we have no rate data for confirmation, this pattern is consistent with an excess of regeneration of NH_4^+ relative to nitrification within the water column and sediments of the river in May, leading to an accumulation of NH_4^+ in the water column (16-24 µM) in May at lower temperatures. At warmer temperatures in July, NH_4^+ did not accumulate in the river (1-4 µM), but NO_3^- was higher (80-164 µM), implying faster rates of nitrification relative to ammonification in summer. The distribution of PO_4^{-3} along the river exhibited a slight maximum (~0.8 µM) near Chester in May, whereas PO_4^{-3} declined steadily from Trenton to Wilmington in July over a significantly higher concentration range.

Chlorophyll *a*

Phytoplankton biomass, as indicated by chlorophyll *a* concentrations (chla), ranged from 2 - 34 µg L^{-1} along RM 71-131 of the river during both May and July 2018 (Figs. 3A-B, middle panels). There was little systematic difference between surface and bottom chla, particularly in the upper river at RM 101-131, and chla also increased downstream from Trenton to Wilmington, reaching higher values in bottom water below RM 131. There were no significant differences in chla between the May and July cruises, but the 2018 chla values are significantly lower than those observed in 2014 in the lower Delaware Bay (Fisher and Gustafson 2015). The values of chla observed in 2018 in the Delaware River are indicative of

borderline eutrophic conditions because many are equivalent to or greater than the chlorophyll *a* criterion of 15 µg L^{-1} derived for Chesapeake Bay based on a variety of associated water quality criteria (Harding et al. 2014).

Because phytoplankton consume nutrients as they increase in biomass, chla is often inversely related to concentrations of NO_3^- and PO_4^{-3}, as was observed on the two cruises in 2014 (Fisher and Gustafson 2015). However, on the two cruises in 2018 in the Delaware River, there were few significant correlations between nutrients and chla (Fig. 4). Chlorophyll *a* concentrations were **positively** correlated with concentrations of NO_3^- in May 2018 ($r^2 = 0.80$, $p<0.01$), suggesting a common origin in the Chester/Wilmington area, possibly from tidal exchange with downstream bay waters.

Dissolved Oxygen

The distributions of dissolved O_2 (DO), chlorophyll a (chla), and respiration (R) along the river are shown for May (Fig. 3A) and July (Fig. 3B). Consistent with the lack of stratification in the Delaware River, there were no significant vertical differences in DO in May or July, although there is a suggestion of lower DO values in bottom water in July at RM 86-116. In May, DO was close to air saturation at 16.5°C, with ~15% undersaturation at RM 116 between Philadelphia and Trenton. In contrast, the July DO data at higher temperatures showed undersaturation of O_2 throughout most of the river (except Trenton), with a maximum undersaturation of ~48% in bottom water near Philadelphia at RM 101.

Respiration

Respiration (R, g O_2 m^{-3} d^{-1}) ranged over -0.06 to -1.02 in both May and July 2018 along RM 71-131 (Tables 1-2, Fig. 3A, B). In May R was significantly higher in bottom waters compared to surface waters of the Delaware River, whereas in July 2018 there were no significant, consistent differences between respiration in surface and bottom waters. There were also no significant differences between R

at the RM stations between May and July, with both sets of data ranging over -0.06 to -1.02 g O_2 m^{-3} d^{-1}. This overlap of respiration rates was also observed for the May and July data of 2014 for the lower Delaware Bay (Fisher and Gustafson 2015).

Along the Delaware River, respiration was distributed in a spatial pattern similar to that of chlorophyll *a*. The overlap of surface and bottom water respiration can be seen in Fig. 5. There were significant correlations between R and chla in both May and July (r^2 = 0.53 -0.35, respectively, Fig. 5), suggesting that much of the respiration was by phytoplankton or by heterotrophic organisms associated with the phytoplankton in the river. An exception is a group of bottom water stations at RM 101-131 with elevated respiration and the lowest chla values. These high respiration values in bottom waters were found in the upper river between Trenton and Philadelphia. In May and July 2014 we also observed strong correlations between respiration and chla in the lower Delaware Bay.

Because respiration was generally related to chlorophyll *a*, we normalized each value of respiration to the observed chlorophyll *a* at each station (Tables 1, 2). This resulted in a community respiration value per unit chlorophyll *a* of phytoplankton (R^B, g O_2 mg $chla^{-1}$ h^{-1}). In our 2014 report on respiration in the lower Delaware Bay, we found that this approach minimized variance in respiration rates; however, in the 2018 data this was not the case, principally because of the elevated respiration in bottom waters of the upper river at the lowest chla concentrations. For comparison with the 2014 lower Bay data, we have retained the computation of R^B in the 2018 data.

Primary Production

There was a strong light dependence of C fixation at a depth z (P_Z, primary production) in the May and July datasets (see examples in Fig. 6). The hyperbolic tangent provided easy parameter estimation for α (g C m^{-3} $(E\ m^{-2})^{-1}$), the light-dependent increase in C fixation with increasing PAR, and for P_m (g C m^{-3} d^{-1}), the light-independent, maximum rate of C fixation (Tables 3A and B, Fig. 6A lower

panel). Five of the 13 river stations were fit well by the hyperbolic tangent function in May 2018, as were 10 of the thirteen river stations in July 2018. The other stations exhibited essentially a linear relationship between C fixation and PAR (Sharp type 1 P vs PAR curves, upper panel of Fig. 6A). At these stations, we obtained good estimates of α, the light-dependent parameter, but it was not possible to estimate P_m because P_Z increased up to the highest PAR available on the incubation day (40 E m^{-2} d^{-1}, in May and 31 E m^{-2} d^{-1} in July, or about 62% of the maximum possible PAR in May and 47% in July, Fisher et al. 2003).

The photosynthetic parameters α and P_m (Tables 3A and B) were more variable in May than in July. The light-dependent parameter α varied over 1-2 orders of magnitude in May (0.003-0.208 g C m^{-3} (E m^{-2})$^{-1}$, with an average ± se = 0.035 ± 0.017 (Table 3A). In contrast, in July 2018 α varied only by a factor of ~2 (0.023-0.052 g C m^{-3} (E m^{-2})$^{-1}$, with an average ± se = 0.038 ± 0.003, Table 3B). A Wilcoxon signed-rank test indicated that the July values of α were not significantly different than the May values at paired stations ($p>0.10$). P_m ranged over 0.13-0.44 g C m^{-3} d^{-1} in May, with an average of 0.33 ± 0.06 (Table 3A); in July the P_m values were similar (range = 0.34 – 0.69, average ± se = 0.52 ± 0.04, Table 3B). A paired t test indicated no significant differences between the two sets of values of P_m at paired stations during May and July.

The photosynthetic parameters α and P_m were significantly correlated. Using data from both May and July, P_m was related to α by an exponential function (Fig. 7, excluding the anomalous data from station RM86-CS, see Fig. 8A). Because of the scatter in the data, the use of an hyperbolic function in Fig. 7 is somewhat arbitrary, and the data can be fit well by linear, exponential and hyperbolic functions. However, despite the statistical uncertainty, a hyperbolic function is consistent with a physiological upper limit to P_m as α increases, and we also observed a clear hyperbolic relationship between P_m and α in the 2014 data (Fisher and Gustafson 2015).

Both α and P_m were influenced by chlorophyll *a* concentrations (Figs. 8A,B). There was a

marginally significant linear correlation between α and chlorophyll *a* in May (r^2 – 0.29, 0.05<p<0.10) and a highly significant relationship in July (r^2 = 0.73, p<0.01, Figs. 8A,B, upper panels). An exception in the May data was station RM86-CS, which showed a very high value of α, almost an order of magnitude higher than all other values of α. One of the next set of stations downriver from RM86-CS (RS71-LS) also had a high calculated α, but the hyperbolic tangent function did not have a significant fit to the data from that station (Table 3A) and was not used in this analysis. This suggests that the phytoplankton population may have been changing in the vicinity of these two stations, but we have insufficient data to substantiate this. For the P_m data in Figs. 8A,B, there was either too few points (Fig. 8A, lower panel) or too small a range of P_m and chlorophyll *a* (Fig. 8B, lower panel) to find significant relationships with chlorophyll *a*.

As we did for the respiration data, we have removed the effect of phytoplankton biomass (chlorophyll *a*) on the photosynthetic parameters. We normalized α and P_m with the observed chlorophyll *a* to create the biomass-specific, light-dependent, photosynthetic parameter α^b with units of g C $(E\ m^{-2})^{-1}$ $(mg\ chla)^{-1}$ and the biomass-specific, light-independent, photosynthetic parameter P_m^b with units of g C $(mg\ chla)^{-1}\ d^{-1}$ (Tables 3A, B). These are useful for comparison with measurements of primary production in other Delaware Bay datasets and in other environments.

There were some effects of the light extinction coefficient k (m^{-1}) on the photosynthetic parameters α, α^b, P_m, and P_m^b. In Fig. 9A, we have plotted both α and α^b as a function of k for both time periods. There was a weak, but significant relationship (r^2 = 0.32, p<0.01) between α and k, and the two months of data clump together with lower values of α (low production per unit light) and k (more transparent water) in May and higher values of α (high production per unit light) and k (more turbid water) in July. This indicates higher values of light-dependent C fixation rates (α) in the more turbid conditions (higher k) in July, suggestive of light adaptation to the higher turbidity. When we removed the effect of chlorophyll *a* on α by plotting α^b versus k, there was no significant relationship that

emerged by month or in the whole 2018 dataset, other than the somewhat higher k values in July. The light-saturated rate of C fixation (P_m) exhibited a positive, linear relationship with k (r^2=0.33, $p<0.05$, Fig. 9B, upper panel). However, the chlorophyll-normalized maximum rate of C fixation P_m^b (Fig. 9B, lower panel) had a smaller range of values (factor of 4) than P_m (factor of 8), and we found a significant, negative, exponential relationship between P_m^b and k (r^2=0.43, $p<0.05$; Fig. 9B, lower panel).

Primary productivity (P, g C m^{-2} d^{-1}) in 2018 ranged over almost an order of magnitude (0.1-0.8 g C m^{-2} d^{-1}, Fig. 10, example in Fig. 6B). There was no significant difference between values of P in May and July (Tables 3A, B), and these P values in 2018 occurred in the lowest range of P values measured in Delaware Bay in 2014 (0.4-6 gC m^{-2} d^{-1}; Fisher and Gustafson 2015). The highest values of P in 2018 occurred at the most downstream stations RM101 to RM71 in May (Table 3A), whereas P was more evenly distributed in July with the highest values in the upper river (Table 3B). Because P was computed using α and P_m, the effects of chla and k on P also emerged, but not for both months (Fig. 10). In the upper panel of Fig. 10 there is an approximately positive, exponential relationship between P and chlorophyll *a* in May, but no significant relationship in July within the same range of P. In contrast, in the lower panel of Fig. 10 there is an inverse exponential relationship (r^2 = 0.94, $p<0.01$) between P and k for July data and a cluster of values for May around the lower range of k. This relationship for P and k in 2018 is similar to a relationship observed in 2014, but within the lowest range of P in that year. As in the 2014 data, the relationships in Figs. 6-10 for the 2018 data potentially provide an empirical basis for estimating the photosynthetic parameters α, P_m, and P using relatively simple field measurements of chlorophyll *a*, k, and PAR.

Conclusions and Synthesis

It is clear that Delaware Bay is nutrient-enriched from its upstream basin. Nitrate, in particular, is quite high in the freshwater end-member (90-170 µM, Fig. 2), similar to the range found in 2014 in mixing curves (100-120 µM, Fisher and Gustafson 2015). These river values are essentially equivalent to concentrations in the Susquehanna River that largely drive eutrophication and hypoxia in the mainstem of Chesapeake Bay (Fisher et al. 1988, Glibert et al. 1995, Kemp et al. 2005). Nutrient concentrations within the Delaware River and Estuary are typically above levels considered saturating for phytoplankton growth, and chlorophyll *a* concentrations generally declined upriver but were often 20-30 mg m^{-3} in the lower river upstream of the turbidity maximum. These chlorophyll a values greater than 15 mg m^{-3} are associated with poor water quality and hypoxia in Chesapeake Bay (Harding et al. 2014). There are also significant correlations between chlorophyll a, nutrients, respiration, and primary production (Figs. 4-5, 8-10) indicating clear linkages between the water column parameters measured in this study.

Rates of both respiration and primary productivity are moderately high in the Delaware River. Why then do we observe so little hypoxia in Delaware Bay compared with Chesapeake Bay? There is some hypoxia, of course, in the Delaware River, particularly in July 2018 (Figs. 3A,B). Both surface and bottom waters were ~10-30% undersaturated in O_2 compared to atmospheric equilibrium, particularly at and just upstream of the Philadelphia/Camden station (RM101). This under-saturation of O_2 indicates regions of net respiration and consumption of organic matter (net heterotrophy) in these river sections. However, compared to the near anoxia of the Chesapeake Bay mainstem and some tributaries in summer (e.g., Hagy et al. 2004), the impact of the nutrients on Delaware Bay is relatively small in terms of dissolved oxygen.

The difference between these two estuarine systems lies in their physics. Chesapeake Bay was over-deepened during the last glacial maximum and is still filling in the former Susquehanna River valley

that we now call Chesapeake Bay. Delaware Bay has access to larger sand supplies which have filled in the former Delaware River valley now known as the lower Delaware estuary. Furthermore, the lower Delaware estuary is shallow and funnel-shaped, amplifying the tidal amplitudes towards the freshwater end. This results in enhanced flushing and mixing energy compared to Chesapeake Bay, which widens from its mouth, resulting in damped tides, less flushing, and low mixing energy in its strongly stratified mid-section. As a result, Chesapeake Bay is density-stratified for much of the year, cutting off the supply of atmospheric O_2 from bottom waters and enhancing hypoxia. In contrast, shallow Delaware Bay is mixed by big tides and is frequently unstratified by density, allowing ventilation of biologically driven oxygen deficits and surpluses in low and high salinity waters, respectively, in both surface and bottom waters, despite the development of relatively high values of phytoplankton biomass. The contrast between these two adjacent estuarine systems is quite striking.

Is the water quality in Delaware Bay cause for concern? In the two time periods examined here (May and July 2018), there were moderate deviations from O_2 atmospheric equilibrium in surface or bottom waters of the upper river, indicating minimal impact on dissolved O_2. We reported similar results from the 2014 data for the estuary downstream from the areas sampled in this report (Fisher and Gustafson 2015). Much of the nutrients appear to be assimilated in the lower bay where the subsequent organic matter is likely subject to dispersal on the continental shelf. Although chlorophyll *a* concentrations at the upper stations of the Delaware River in 2018 were moderately high (20-30 mg m^{-3}), in May 2014 chlorophyll a concentrations exceeded 100 mg m^{-3} in the Delaware Estuary (Fisher and Gustafson 2015). Values of that magnitude are often associated with harmful algal blooms, which can have significant impacts on fisheries, recreational activities, and human health (Harding et al. 2014). Reducing nutrient inputs in the upper estuary and in the river basin would reduce the potential for harmful algal blooms in the lower bay.

References

Bevington, P. R. 1969. Data Reduction and Error Analysis for the Physical Sciences. McGraw-Hill Book Co., NY, 336 pps.

Colt, J. 1984. Computation of dissolved gas concentrations in water as functions of temperature, salinity, and pressure. Amer. Fish. Soc. Spec. Pub. 14

Fisher, T. R., L. W. Harding, D. W. Stanley, and L. G. Ward. 1988. Phytoplankton, nutrients, and turbidity in the Chesapeake, Delaware, and Hudson River estuaries. Est. Coastal Shelf Sci. 27: 61-93

Fisher, T. R., J. M. Melack, J. Grobbellar, and R. W. Howarth. 1995. Nutrient limitation of phytoplankton and eutrophication of estuarine and marine waters. pps. 301-322 IN: H. Tiessen (ed.) Phosphorus cycling in Terrestrial and Aquatic Ecosystems. SCOPE, Wiley.

Fisher, T. R., A. B. Gustafson, K. Sellner, R. Lacuture, L. W. Haas, R. Magnien, R. Karrh, and B. Michael. 1999. Spatial and temporal variation in resource limitation in Chesapeake Bay. Mar. Biol. 133: 763-778

Fisher, T. R., A. B. Gustafson, G. R. Radcliffe, K. L. Sundberg, and J. C. Stevenson. 2003. A long-term record of photosynthetically active radiation (PAR) and total solar energy at 38.6° N, 78.2° W. Estuaries 26: 1450-1460

Fisher, T. R. and A. B. Gustafson. 2015. Concentrations of nutrients and chlorophyll a, and rates of respiration and primary production in samples from Delaware Bay collected in May and July 2014. Rep. DRBC, May 2015

Glibert, P. M., D. J. Conley, T. R. Fisher, L. W. Harding, Jr., and T. C. Malone. 1995. Dynamics of the 1990 winter/spring bloom in Chesapeake Bay. Mar. Ecol. Prog. Ser. 122:27-43

Hagy, J. D., W. R. Boynton, C. W. Keefe, and K. V. Wood. 2004. Hypoxia in Chesapeake Bay, 1950-2001: long-term change in relation to nutrient loading and river flow. Estuaries 27: 634-658

Harding, Jr., L. W., R. A. Batiuk, T. R. Fisher, C. L. Gallegos, T. C. Malone, W. D. Miller, M. R. Mulholland, H. W. Paerl, and P. Tango. 2014. Scientific bases for numerical chlorophyll criteria in Chesapeake Bay. Estuaries and Coasts 37: 134-148

Jassby, A. D. and T. Platt 1976. Mathematical formulation of the relationship between photosynthesis and light for phytoplankton. Limnol. Oceanogr. 21: 540-547

Kana, T. M., C. Darkangelo, M. D. Hunt, J. B. Oldham, G. E. Bennett, and J. C. Cornwell. 1994. Membrane inlet mass spectrometer for rapid high-precision determination of N_2, O_2, and Ar in environmental water samples. Anal. Chem. 66:4166-4170

Kemp, W. M., W. R. Boynton, J. E. Adolf, D. F. Boesch, W. C. Boicourt, G. Brush, J. C. Cornwell, T. R. Fisher, P. M. Glibert, J. D. Hagy, L. W. Harding, E. D. Houde, D. G. Kimmel, W. D. Miller, R. I. E. Newell, M. R. Roman, E. M. Smith, J. C. Stevenson. 2005. Eutrophication of Chesapeake Bay: Historical trends and ecological interactions. Mar. Ecol. Prog. Ser. 303: 1-29

Lane, L., S. Rhoades, C. Thomas, and L. Van Heukelem. 2000. Standard Operating Procedures of the Analytical Services Laboratory of the Horn Point Laboratory, Center for Environmental Science, University of Maryland. Tech. Rep. No. TS-264-00

Sharp, J. H., K. Yoshiyama, A. E. Parker, M. C. Schwartz, S. E. Curless, A. Y. Beauregard, J. E. Ossolinkski, and A. R. Davis. 2009. A biogeochemical view of estuarine Eutrophication: seasonal and spatial trends and correlations in the Delaware Estuary. Estuaries and Coasts 32: 1023-1043

Sharp, J. H. 2013. Biogeochemical Methods Manual. School of Marine Science and Policy, College of Earth, Ocean, and Environment, University of Delaware.

Table 1. Summary of salinity, temperature, oxygen, nutrients, chlorophyll *a* , and respiration in the water column of the Delaware River on 8 May 2018. RMxxx refers to River Mile upstream from a line between Cape Henlopen and Cape May. Highlighted stations are a block between Trenton and Philadelphia with elevated respiration (>0.5 gO_2 m^{-3} d^{-1}) in bottom water.

			mg O_2 L^{-1}		µM		Chla, mg m^{-3}		mg O_2 L^{-1} d^{-1}		g O_2 (mg chla)$^{-1}$ d^{-1}	
Station	Salinity	Temp ◦C	DO	NH_4	NO_3	PO_4	ave	se	respiration (R)	se	R^b	se
RM131-LS top	0.113	16.56	9.49	3.9	58.1	0.47	6.04	0.09	-0.207	0.133	-0.034	0.022
RM131-CS top	0.113	16.48	9.35	4.17	58.00	0.69	4.37	0.43	-0.304	0.004	-0.070	0.007
RM131-RS top	0.112	16.47	9.36	3.01	56.90	0.67	3.95	0.93	-0.069	0.154	-0.017	0.039
RM116-LS top	0.105	17.50	9.53	6.15	47.20	0.58	3.78	0.04	-0.255	0.146	-0.068	0.039
RM116-CS top	0.105	17.98	8.33	6.72	47.20	0.64	3.31	0.06	-0.249	0.019	-0.075	0.006
RM116-RS top	0.108	17.77	8.50	6.71	47.50	0.63	2.59	0.11	-0.266	0.007	-0.103	0.005
RM101-LS top	0.119	16.21	9.00	13.80	52.90	0.78	7.81	0.09	-0.336	0.064	-0.043	0.008
RM101-CS top	0.122	16.30	8.85	16.50	53.90	0.74	7.24	0.49	-0.055	0.263	-0.008	0.036
RM86-LS top	0.153	16.41	9.34	16.50	84.70	0.82	21.84	1.07	-0.638	0.184	-0.029	0.009
RM86-CS top	0.153	16.23	9.01	18.60	85.00	0.84	18.55	0.71	-0.427	0.128	-0.023	0.007
RM86-RS top	0.152	16.63	9.09	20.20	85.40	0.82	18.24	0.13	0.335	0.208	0.018	-0.011
RM71-CS top	0.158	16.26	9.37	10.90	94.60	0.72	12.74	0.76	-0.313	0.084	-0.025	0.007
RM71-LS top	0.153	16.39	9.77	3.04	93.70	0.50	22.94	1.11	-0.183	0.028	-0.008	0.001
RM131-LB botton	0.112	16.39	9.28	3.44	54.70	0.62	6.44	0.05	-0.098	0.037	-0.015	0.006
RM131-CB bottom	0.112	16.43	9.33	3.29	56.40	0.71	4.21	0.25	-0.102	0.024	-0.024	0.006
RM131-RB bottom	0.112	16.47	9.36	3.33	55.70	0.65	4.03	0.03	-0.673	0.133	-0.167	0.033
RM1116-LB botton	0.105	17.43	8.36	5.90	46.40	0.74	3.68	0.41	-0.639	0.055	-0.174	0.024
RM116-CB bottom	0.108	17.62	8.19	6.89	46.40	0.70	2.63	0.15	-0.606	0.020	-0.231	0.015
RM116-RB bottom	0.111	17.67	8.32	7.13	48.00	0.74	2.44	0.12	-0.882	0.049	-0.361	0.026
RM101-LB bottom	0.120	16.16	8.98	14.20	56.00	0.79	9.05	0.22	-0.643	0.036	-0.071	0.004
RM101-CB bottom	0.123	16.15	8.60	17.85	54.10	0.67	6.35	0.23	-0.696	0.055	-0.110	0.009
RM86-LB bottom	0.153	16.38	9.50	16.80	86.10	0.66	26.90	0.54	-0.679	0.190	-0.025	0.007
RM86-CB bottom	0.153	16.31	8.93	18.20	87.90	0.73	20.42	0.89	-0.793	0.177	-0.039	0.009
RM86-RB bottom	0.154	16.40	8.87	24.10	88.40	1.00	19.22	0.84	-0.401	0.340	-0.021	0.018
RM71-CB bottom	0.159	16.23	9.57	9.36	95.90	0.79	15.14	0.14	-0.395	0.102	-0.026	0.007
RM71-LB bottom	0.153	16.27	10.82	2.19	95.65	0.62	34.08	1.95	-0.560	0.122	-0.016	0.004
minimum =	0.105	16.15	8.19	2.19	46.4	0.47	2.44	0.03	-0.882		-0.361	
maximum =	0.159	17.98	10.82	24.10	95.9	1.00	34.08	1.95	0.335		0.018	
average =	0.129	16.66	9.12	10.11	66.8	0.70	11.07	0.45	-0.390		-0.068	
std. error =	0.004	0.11	0.11	1.30	3.7	0.02	1.75	0.09	0.055		0.016	

Table 2. Summary of salinity, temperature, oxygen, nutrients, chlorophyll *a*, and respiration in the water column of the Delaware River on 9 July 2018. RMxxx refers to River Mile upstream from a line between Cape Henlopen and Cape May.

			mg O_2 L^{-1}		µM		Chla, mg m^{-3}		g O_2 m^{-3} d^{-1}		g O_2 (mg Chla)$^{-1}$ d^{-1}	
Station	Salinity	Temp ◦C	DO	NH_4	NO_3	PO_4	ave	se	respiration	se	R^B	se
RM131-LS top	0.126	25.48	8.08	3.98	80.0	2.05	4.17	0.09	-0.431	0.055	-0.103	-0.013
RM131-CS top	0.126	25.53	8.06	2.00	79.2	2.04	4.26	0.06	-0.529	0.066	-0.124	-0.015
RM131-RS top	0.125	25.63	8.08	1.37	77.1	1.95	3.82	0.21	-0.368	0.013	-0.096	-0.006
RM116-LS top	0.121	27.51	6.23	1.26	76.2	1.95	16.64	0.22	-0.519	0.060	-0.031	-0.004
RM116-CS top	0.121	27.59	6.42	1.69	77.2	2.03	13.01	0.14	-0.599	0.055	-0.046	-0.004
RM116-RS top	0.121	27.59	7.75	1.73	76.6	2.03	12.92	0.05	-0.861	0.030	-0.067	-0.002
RM101-LS top	0.152	26.57	5.87	0.81	117.0	1.88	14.91	0.53	-0.698	0.067	-0.047	-0.005
RM101-CS top	0.155	26.59	5.09	0.72	119.0	1.93	13.27	0.22	-0.394	0.050	-0.030	-0.004
RM86-LS top	0.170	26.53	7.19	0.78	161.0	1.69	15.18	0.36	-0.533	0.032	-0.035	-0.002
RM86-CS top	0.170	26.58	6.80	0.83	161.5	1.33	9.99	0.32	-0.430	0.028	-0.043	-0.003
RM86-RS top	0.171	26.52	6.59	0.75	166.0	1.72	11.98	1.60	-0.374	0.035	-0.031	-0.005
RM71-CS top	0.291	27.02	7.09	0.63	143.0	1.35	12.16	1.15	-0.402	0.087	-0.033	-0.008
RM71-LS top	0.218	26.66	7.07	0.67	146.0	1.37	11.50	0.14	-0.415	0.042	-0.036	-0.004
RM131-LB bottom	0.129	25.51	7.92	2.24	81.6	1.99	3.98	0.32	-0.287	0.022	-0.072	-0.008
RM131-CB bottom	0.125	25.53	8.06	1.21	79.6	1.99	2.98	0.02	-0.218	0.035	-0.073	-0.012
RM131-RB bottom	0.125	25.61	8.05	1.48	79.4	1.90	3.37	0.15	-0.118	0.061	-0.035	-0.018
RM116-LB bottom	0.121	27.50	5.90	1.65	78.5	2.03	--	--	-0.519	0.231	--	--
RM116-CB bottom	0.121	27.59	5.75	1.53	78.4	1.94	11.01	0.45	-0.528	0.272	-0.048	-0.025
RM116-RB bottom	0.121	27.58	5.59	1.83	78.5	1.98	13.49	0.36	-0.859	0.040	-0.064	-0.003
RM101-LB bottom	0.154	26.56	5.35	1.01	115.5	1.78	15.27	0.36	-0.238	0.017	-0.016	-0.001
RM101-CB bottom	0.156	26.58	4.30	0.90	120.0	1.75	12.25	0.53	-0.402	0.244	-0.033	-0.020
RM86-LB bottom	0.171	26.36	6.12	0.95	158.0	1.48	19.71	0.53	-0.489	0.032	-0.025	-0.002
RM86-CB bottom	0.170	26.51	5.91	0.95	160.0	1.80	24.23	1.51	-1.018	0.145	-0.042	-0.007
RM86-RB bottom	0.171	26.48	6.18	0.85	162.0	1.75	13.76	0.09	-0.836	0.075	-0.061	-0.005
RM71-CB bottom	0.295	26.68	6.57	1.14	143.0	1.51	11.90	0.18	-0.760	0.020	-0.064	-0.002
RM71-LB bottom	0.220	26.56	6.86	0.95	145.0	1.47	12.61	0.18	-0.697	0.036	-0.055	-0.003
minimum =	0.121	25.48	4.30	0.63	76.2	1.33	2.98	0.02	-1.018		-0.124	
maximum =	0.295	27.59	8.08	3.98	166.0	2.05	24.23	1.60	-0.118		-0.016	
average =	0.159	26.57	6.65	1.30	113.8	1.80	11.53	0.39	-0.520		-0.052	
std. error =	0.010	0.14	0.21	0.14	7.1	0.05	1.06	0.08	0.043		0.005	

Table 3A. Primary Production Parameters: 19 May 2018. Abbreviations: r^2 = coefficient of determination, p = probability due to chance, α = initial slope of light-dependent primary production, α^b = α normalized to chlorophyll a, P_m = maximum rate of primary production, $P_m{}^b$ = P_m normalized to chloroph k = light extinction coefficient in the water column, and P = primary productivity (integrated rate of C fixation in the water column).

Sample	r^2	regression p	$gC\ m^{-3}\ (E\ m^{-2})^{-1}$ α	p(α)	$gC\ (E\ m^{-2})^{-1}\ (mg\ chla)^{-1}$ α^b	$gC\ m^{-3}\ d^{-1}$ P_m	p(P_m)	$gC\ (mg\ chla)^{-1}\ d^{-1}$ $P_m{}^b$	ext. coef. k, m^{-1}	$gC\ m^{-2}\ d^{-1}$ P
RM131-LS	0.91	<0.01	0.00418 ± 0.00080	<0.01	0.0007	NA	--	--	1.27	0.258
RM131-CS	0.95	<0.01	0.00349 ± 0.00035	<0.01	0.0008	NA	--	--	1.33	0.230
RM131-RS	0.93	<0.01	0.00970 ± 0.00168	<0.01	0.0025	0.126 ± 0.016	<0.01	0.0319	2.22	0.141
RM116-LS	0.99	<0.01	0.0153 ± 0.0009	<0.01	0.0040	0.307 ± 0.016	<0.01	0.0812	1.50	0.424
RM116-CS	0.99	<0.01	0.00690 ± 0.00050	<0.01	0.0021	NA	--	--	1.22	0.361
RM116-RS	0.92	<0.01	0.00399 ± 0.00068	<0.01	0.0015	NA	--	--	3.60	0.111
RM101-LS	0.91	<0.01	0.0123 ± 0.0022	<0.01	0.0016	NA	--	--	2.71	0.449
RM101-CS	0.98	<0.01	0.0239 ± 0.0023	<0.01	0.0033	0.434 ± 0.024	<0.01	0.0599	1.23	0.748
RM86-LS	0.95	<0.01	0.0194 ± 0.0025	<0.01	0.0009	NA	--	--	1.73	1.053
RM86-CS	0.97	<0.01	0.119 ± 0.018	<0.01	0.0064	0.436 ± 0.022	<0.01	0.0235	3.42	0.471
RM86-RS	0.80	<0.05	0.0142 ± 0.0041	<0.05	0.0008	NA	--	--	2.48	0.781
RM71-CS	0.80	<0.05	0.0125 ± 0.0036	<0.05	0.0010	NA	--	--	2.55	0.683
RM71-LS	0.54	>0.10	0.208 ± 0.084	>0.10	0.0091	0.364 ± 0.043	>0.10	0.0317	2.24	0.695
minimum =			0.003		0.0007	0.126		0.0235	1.22	0.111
maximum =			0.208		0.0091	0.436		0.0812	3.60	1.053
average =			0.035		0.0021	0.333		0.0456	2.11	0.476
std. error =			0.017		0.0007	0.057		0.0242	0.23	0.078

Table 3B. Primary Production Parameters: July 2018. Abbreviations: r^2 = coefficient of determination, p = probability due to chance, α = initial slope of light-dependent primary production, α^b = α normalized to chlorophyll a, P_m = maximum rate of primary production, P_m^b = Pm normalized to chlorophyll a, k = water column light extinction coefficient, and P = primary productivity (integrated rate of C fixation in the water column).

Sample	r^2	regression p	gC m^{-3} (E m^{-2})$^{-1}$ α	p(α)	gC (E m^{-2})$^{-1}$ (mg chla)$^{-1}$ α^b	gC m^{-3} d^{-1} P_m	p(P_m)	gC (mg chla)$^{-1}$ d^{-1} P_m^b	ext. coef. k, m^{-1}	gC m^{-2} d^{-1} Prim. Prod.
RM131-LS	0.99	<0.01	0.0232 ± 0.0010	<0.01	0.0056	NA	--	--	3.55	0.308
RM131-CS	0.99	<0.01	0.0222 ± 0.0010	<0.01	0.0052	NA	--	--	1.46	0.768
RM131-RS	0.99	<0.01	0.0232 ± 0.0007	<0.01	0.0061	NA	--	--	3.66	0.315
RM116-LS	0.99	<0.01	0.0521 ± 0.0091	<0.01	0.0031	0.614 ± 0.087	<0.01	0.0369	5.69	0.247
RM116-CS	0.98	<0.01	0.0447 ± 0.0045	<0.01	0.0034	0.668 ± 0.065	<0.01	0.0513	1.97	0.688
RM116-RS	0.98	<0.01	0.0471 ± 0.0055	<0.01	0.0036	0.687 ± 0.076	<0.01	0.0532	4.83	0.292
RM101-LS	0.98	<0.01	0.0441 ± 0.0075	<0.01	0.0030	0.406 ± 0.048	<0.01	0.0272	3.07	0.333
RM101-CS	0.87	<0.01	0.0342 ± 0.0020	<0.01	0.0026	0.547 ± 0.033	<0.01	0.0412	4.84	0.198
RM86-LS	0.92	<0.01	0.0401 ± 0.0077	<0.01	0.0026	0.416 ± 0.059	<0.01	0.0274	3.34	0.302
RM86-CS	0.96	<0.01	0.0417 ± 0.0056	<0.01	0.0042	0.341 ± 0.029	<0.01	0.0341	2.99	0.297
RM86-RS	0.94	<0.01	0.0467 ± 0.0083	<0.01	0.0039	0.419 ± 0.051	<0.01	0.0350	2.39	0.445
RM71-CS	0.96	<0.01	0.0392 ± 0.0080	<0.01	0.0032	0.491 ± 0.061	<0.01	0.0404	4.47	0.243
RM71-LS	0.88	<0.01	0.0292 ± 0.0076	<0.01	0.0025	0.606 ± 0.217	>0.10	0.0527	4.90	0.222
minimum =			0.0232		0.0025	0.341		0.0272	1.97	0.198
maximum =			0.0521		0.0061	0.687		0.0532	5.69	0.688
average =			0.0375		0.0038	0.520		0.0399	3.63	0.358
std. error =			0.0028		0.0003	0.039		0.0031	0.35	0.049

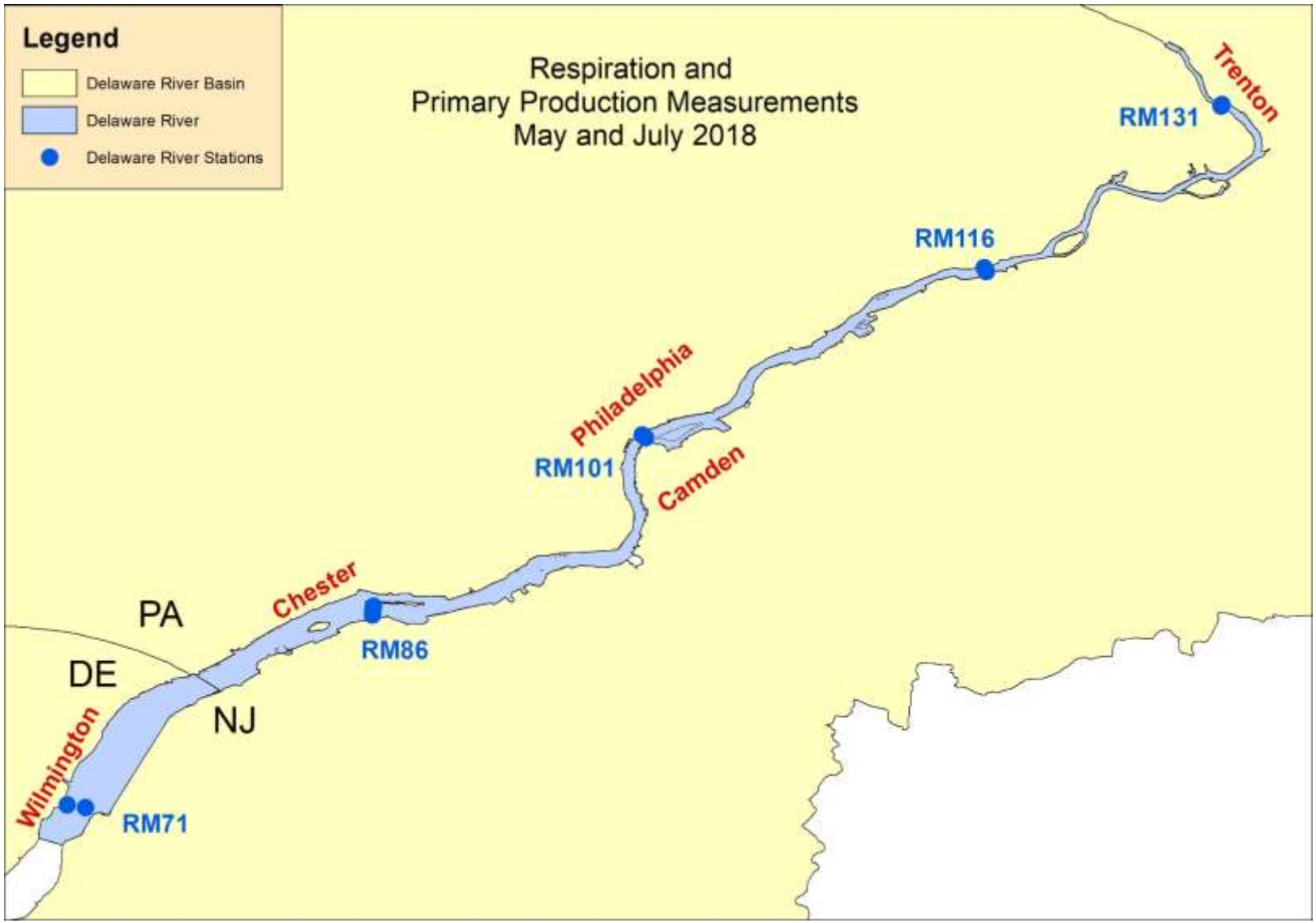

Figure 1. Map of sampling locations in the Delaware River at River Mile (RM) 71 to 131 in May and July 2018.

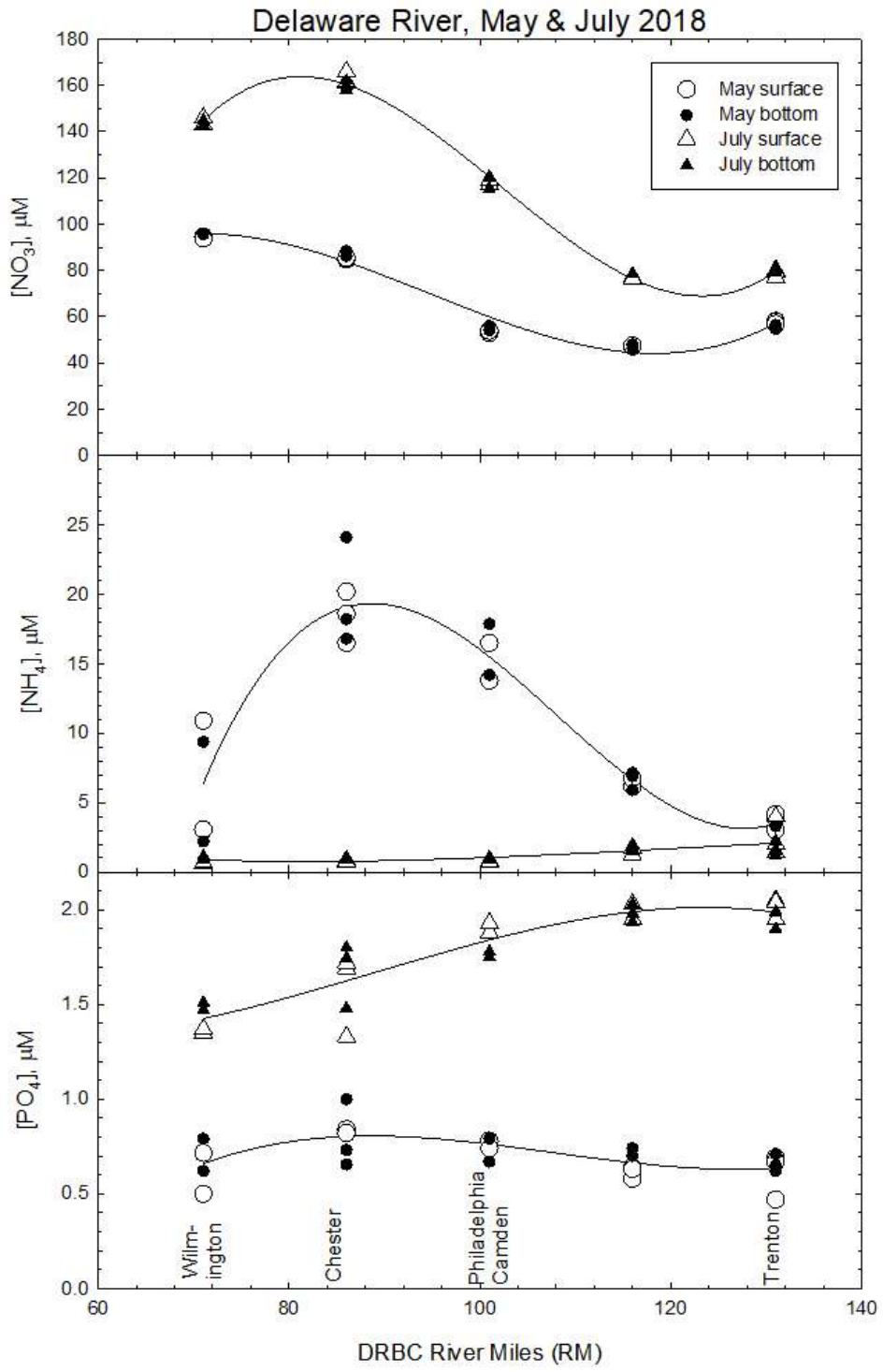

Figure 2. Distribution of nitrate (NO_3), ammonium (NH_4), and phosphate (PO_4) in surface and bottom waters of the Delaware River. There were no consistent significant differences between surface and bottom concentrations, and lines were fit to all data from each river station. Symbols differ in size only to show overlapping values.

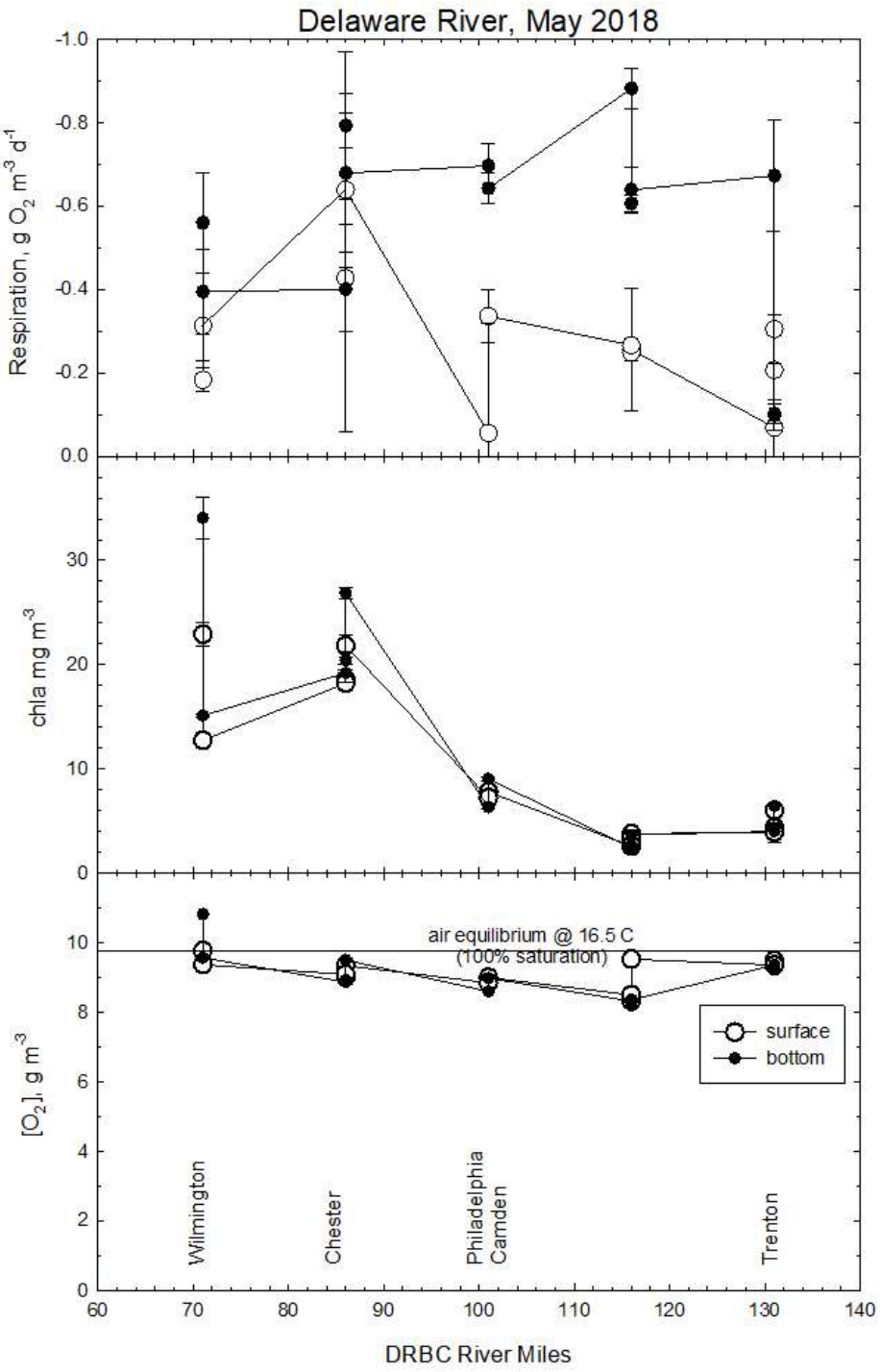

Figure 3A. Respiration, chlorophyll *a*, and dissolved O_2 in the Delaware River in May 2018. Respiration in the upper river (RM101-131) was elevated compared to the lower river, and oxygen was slightly undersaturated in this area of the river. Air equilibrium for O_2 was calculated from temperature and salinity using Colt (1984).

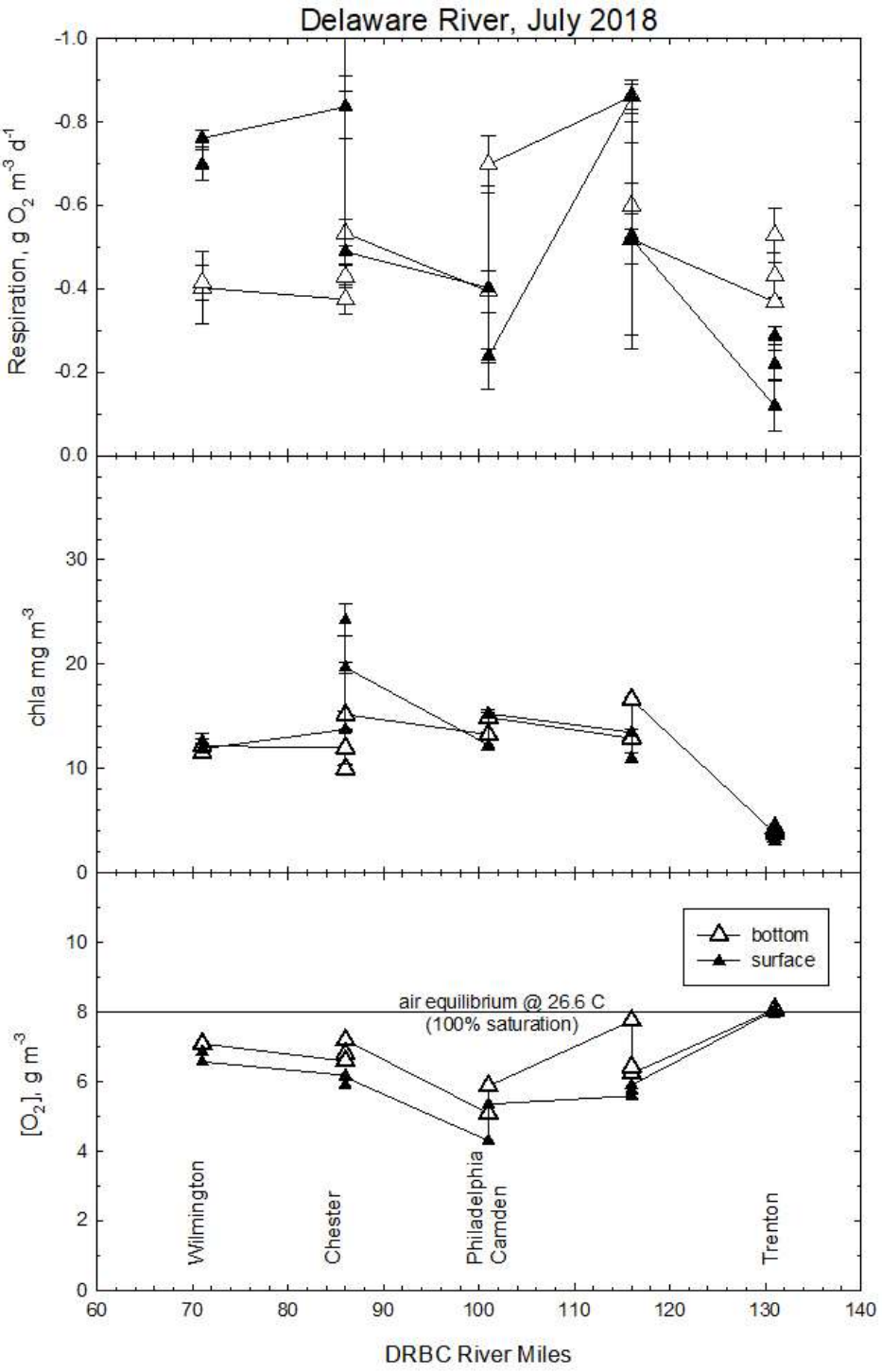

Figure 3B. Respiration, chlorophyll a, and dissolved O_2 in the Delaware River in July 2018. Chlorophyll *a* and respiration values were similar to those of May, but there was a larger oxygen deficit in July in both surface and bottom waters. Air equilibrium for O_2 was calculated from temperature and salinity using Colt (1984).

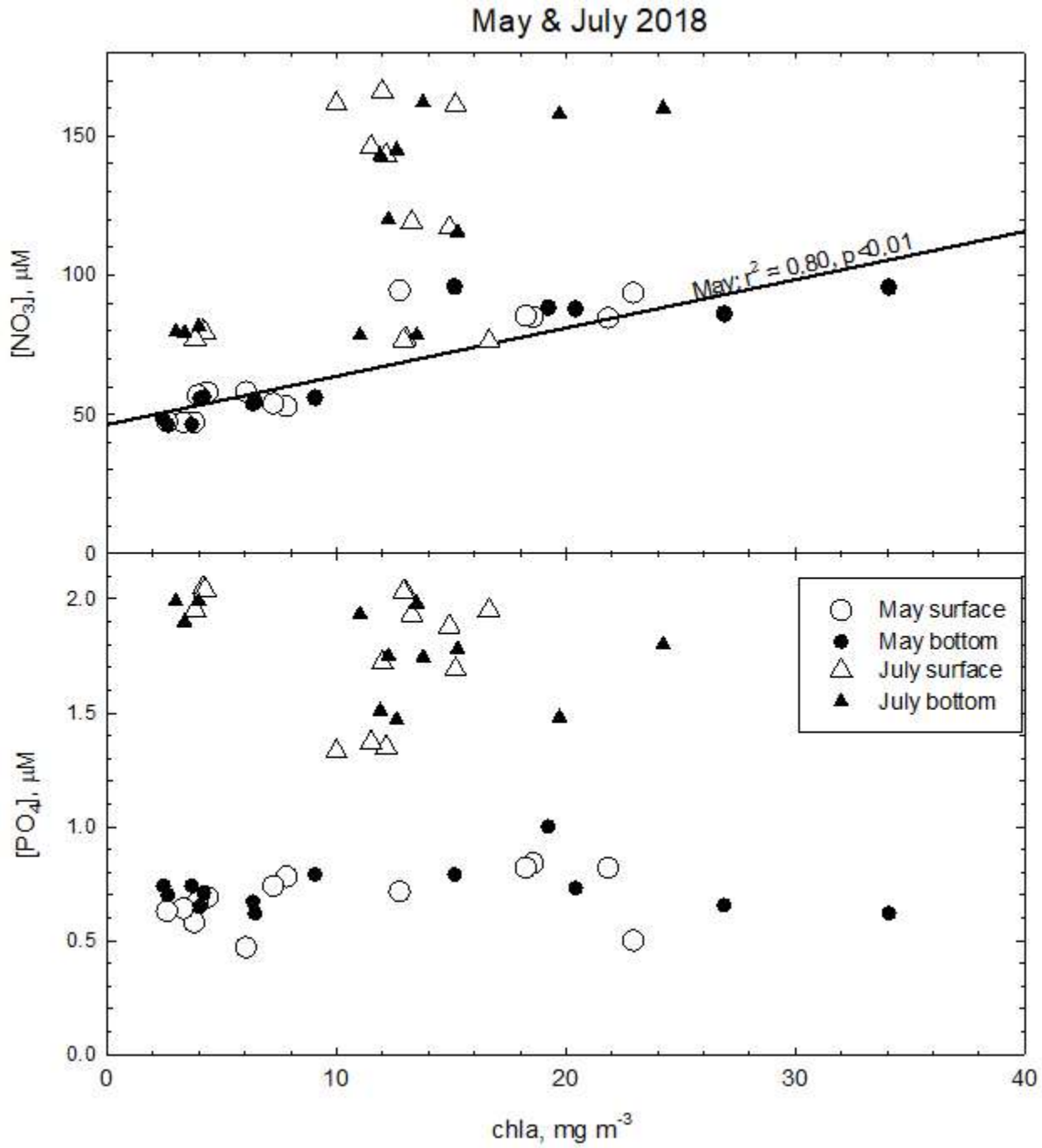

Figure 4. Relationships of chlorophyll *a* with nitrate (NO_3) and phosphate (PO_4) concentrations in the two time periods. Phosphate was independent of chlorophyll *a* concentrations, but in May there was a positive linear relationship with nitrate.

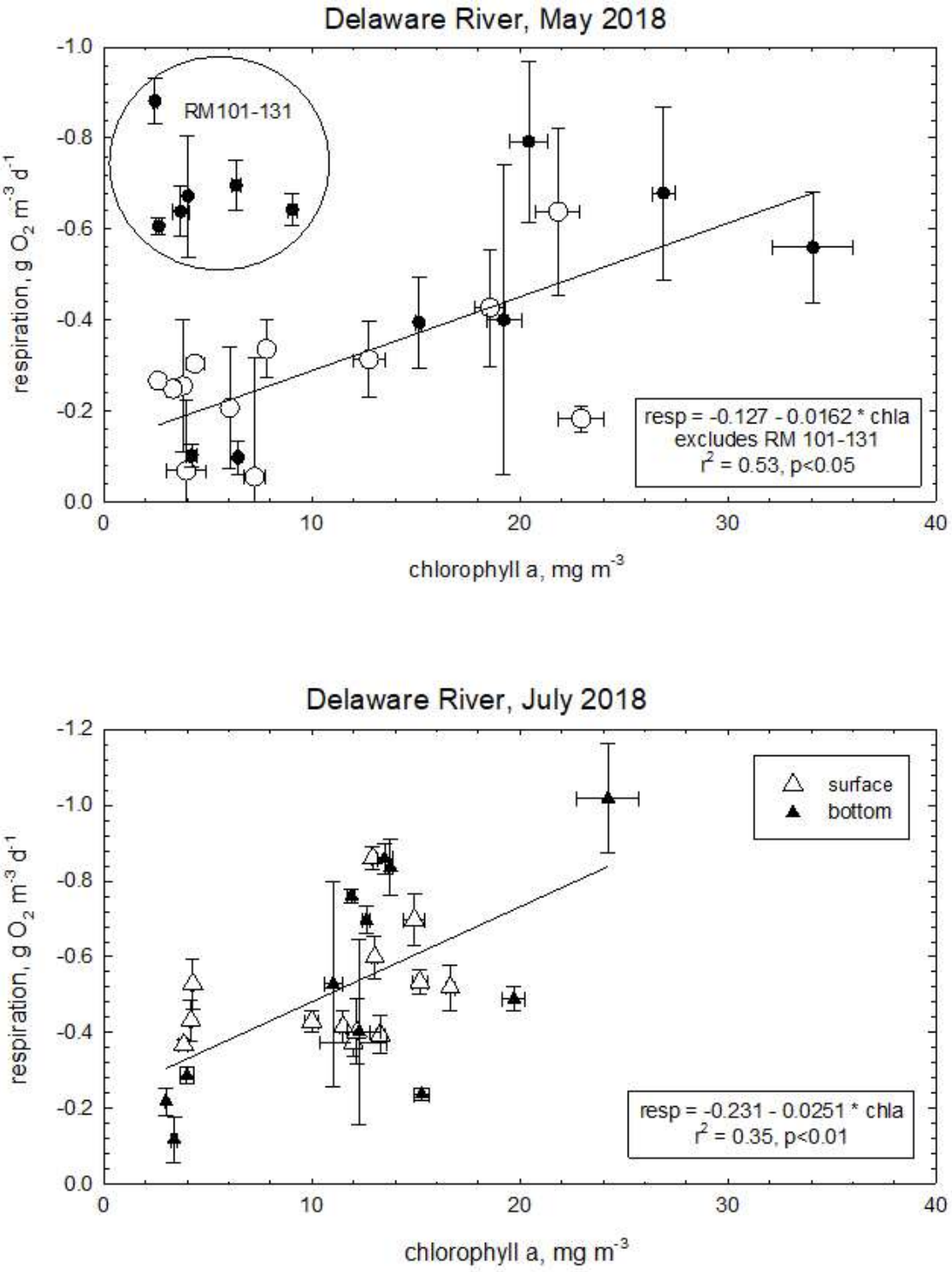

Figure 5. Respiration as a function of chlorophyll a in the Delaware River for May and July 2018. Respiration was positively correlated with river chlorophyll *a*, except in bottom waters of the upper river in May 2018, when respiration in bottom waters was elevated at relatively low chlorophyll a.

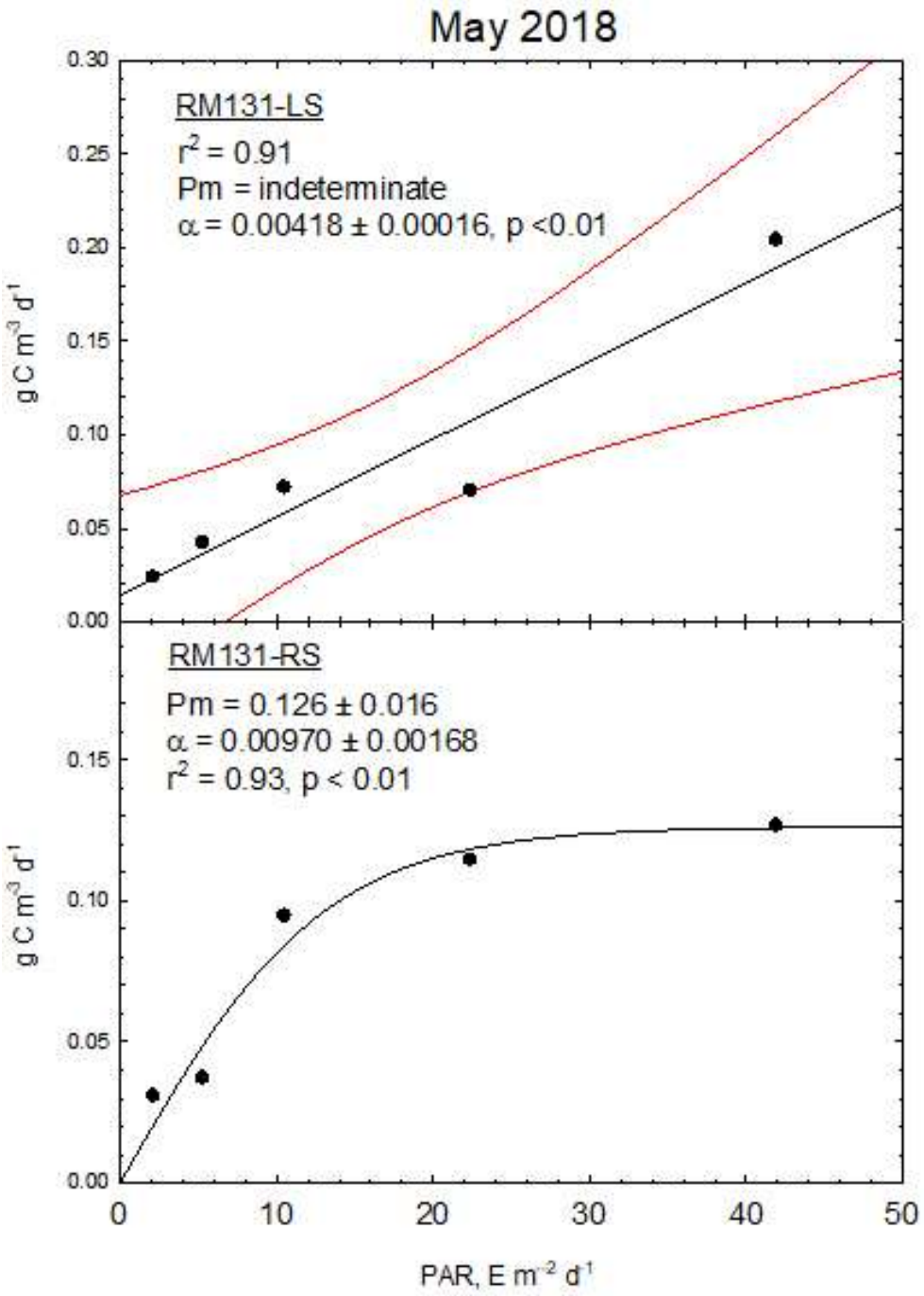

Figure 6A. Two examples of the hyperbolic tangent fit of eq. 7 to production vs PAR data. The top panel is essentially a linear response to PAR (Sharp type 1). The initial linear response to PAR, α, was estimated, but P_m, the maximum rate of primary production, could not be determined in this example. The bottom panel is an example where primary production was essentially saturated by PAR at PAR > 20 E m^{-2} d^{-1} (Sharp type 2), and both α and P_m were estimated. There were no examples of Sharp type 3 (light inhibition) in this dataset. Red curved lines are 95% confidence intervals.

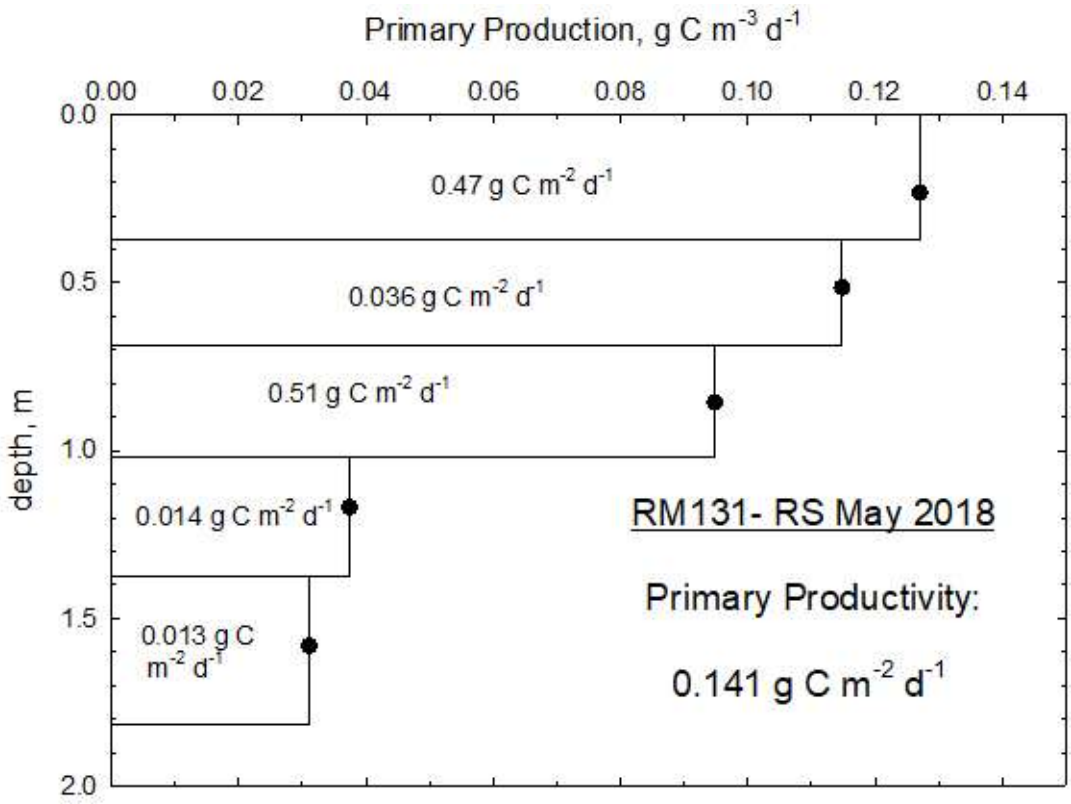

Figure 6B. Example of depth integration to obtain integrated primary productivity (P, g C m^{-2} d^{-1}) at each station from the individual measurements of primary production (P_Z, g C m^{-3} d^{-1}) at fixed light depths of 3-60% ambient light. Light depths (I_Z/I_0) were converted to water column depths using the measured extinction coefficient (k, m^{-1}) at each station (eq. 8), and primary productivity in each depth interval (ΔZ) was computed as $P_Z * \Delta Z$ and summed vertically for the total station primary productivity (eq. 9).

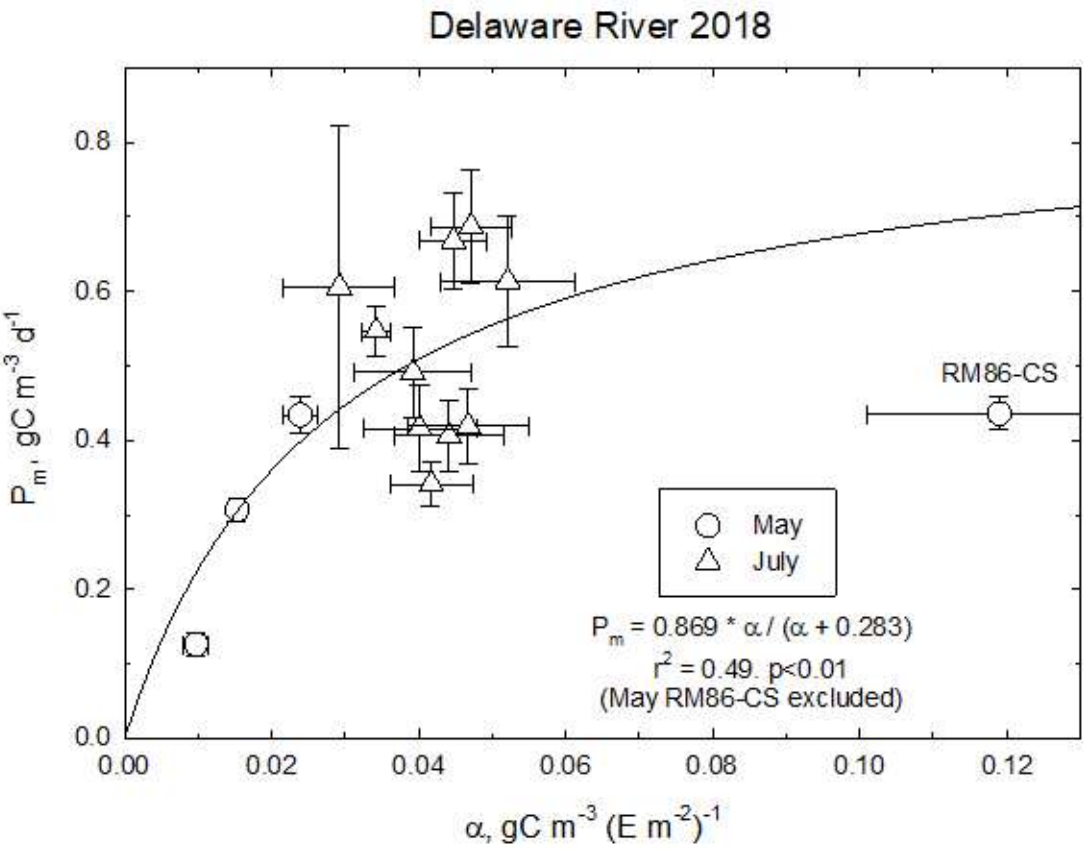

Figure 7. Relationship between the two photosynthetic parameters P_m (light-saturated primary production) and α (light-dependent primary production) in May and July 2018 in the Delaware River stations. Data from station RM86-CS was excluded from the hyperbolic curve.

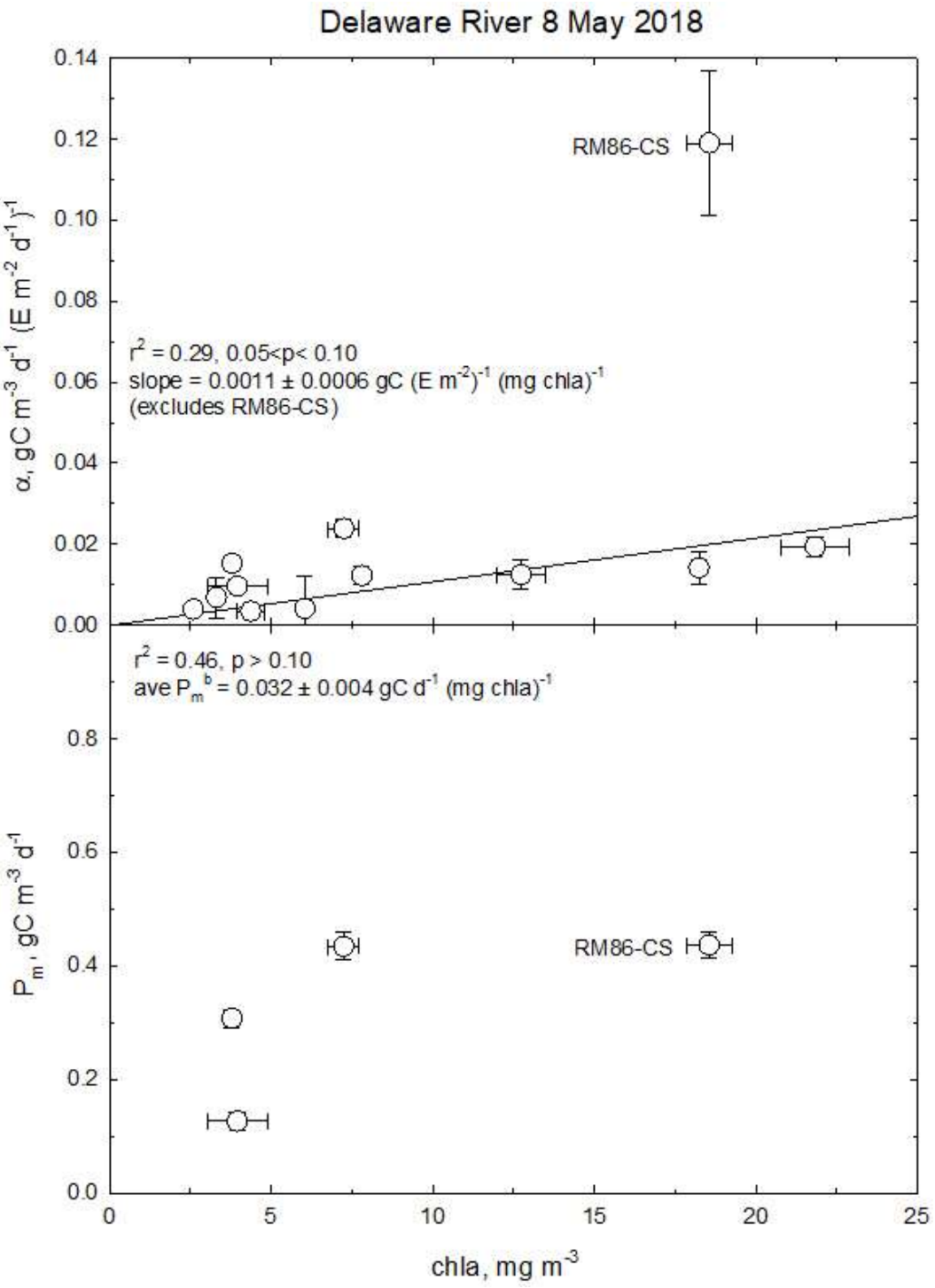

Figure 8A.Relationship between the photosynthetic parameters α and P_m to chlorophyll *a* (chla) in May 2018 at river mile stations (RM) on the Delaware River.

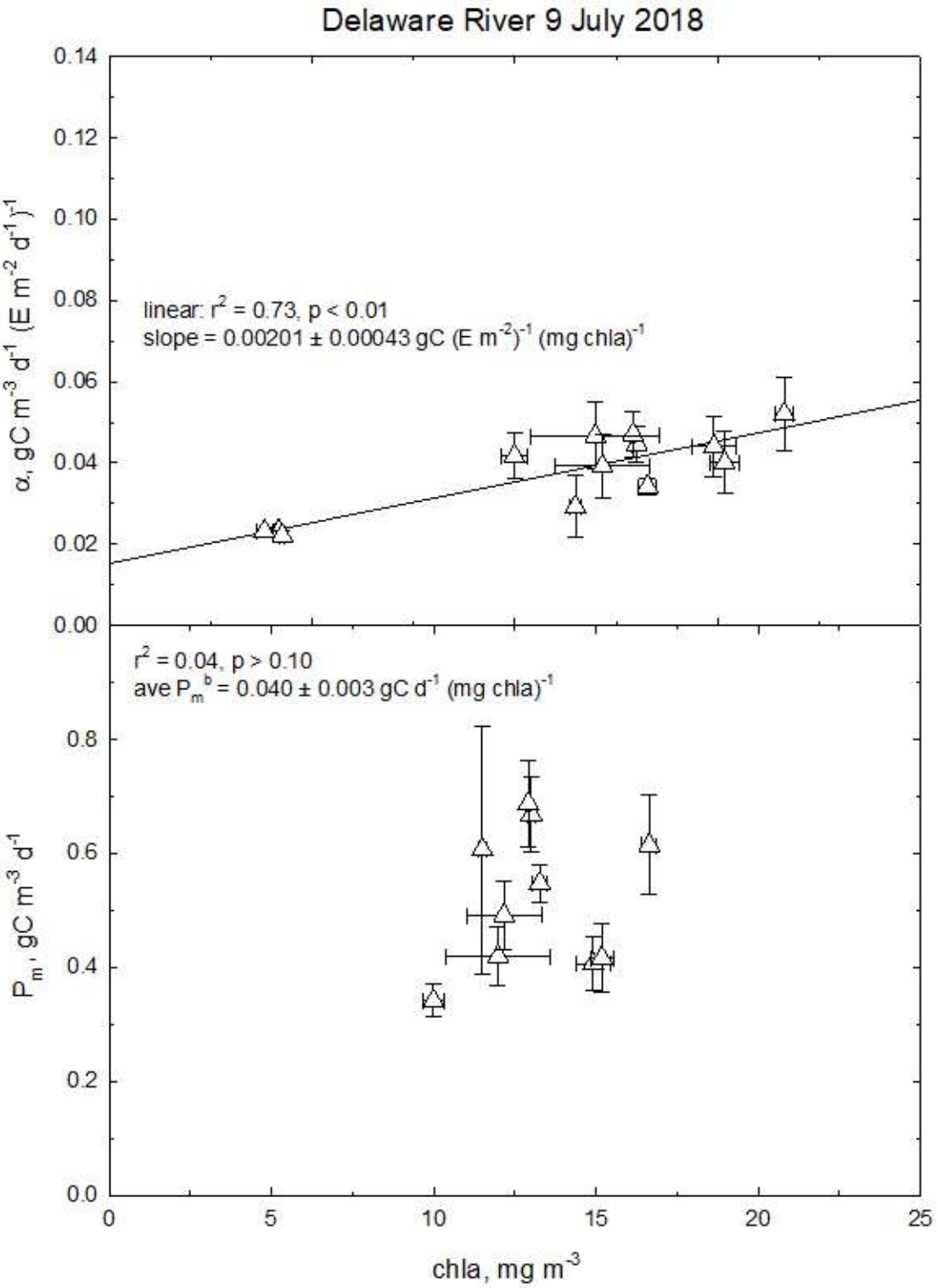

Figure 8B. Relationship between the photosynthetic parameters α and P_m to chlorophyll *a* (chla) in July 2018 at river mile stations (RM) in Delaware Bay.

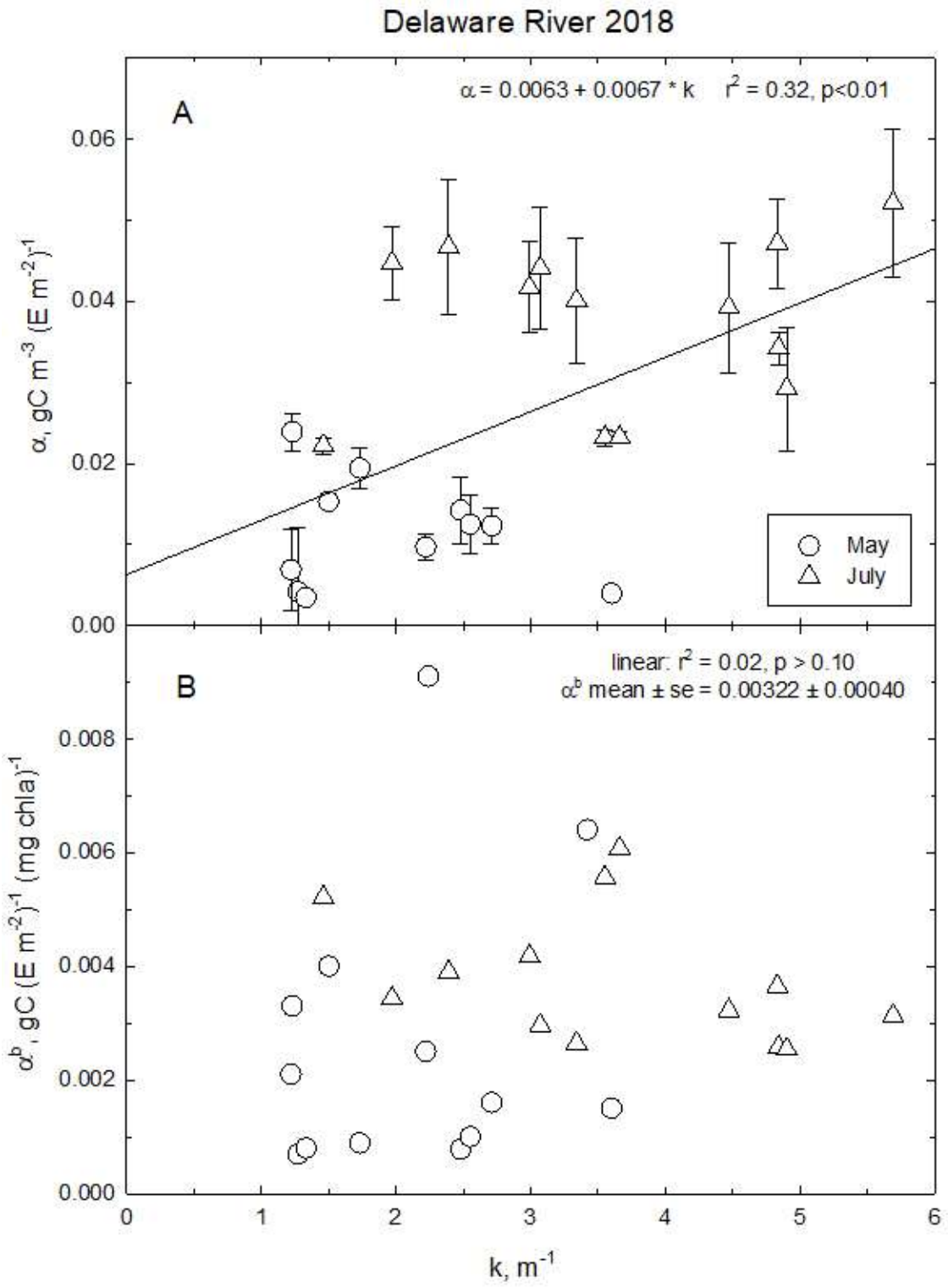

Figure 9A. The relationship of the light-dependent photosynthetic parameters α and α^b to the water column extinction coefficient for PAR (k). There were no significant effects of k on α^b in the lower panel, but α had a significant, linear relationship with k (upper panel) for the combined dataset.

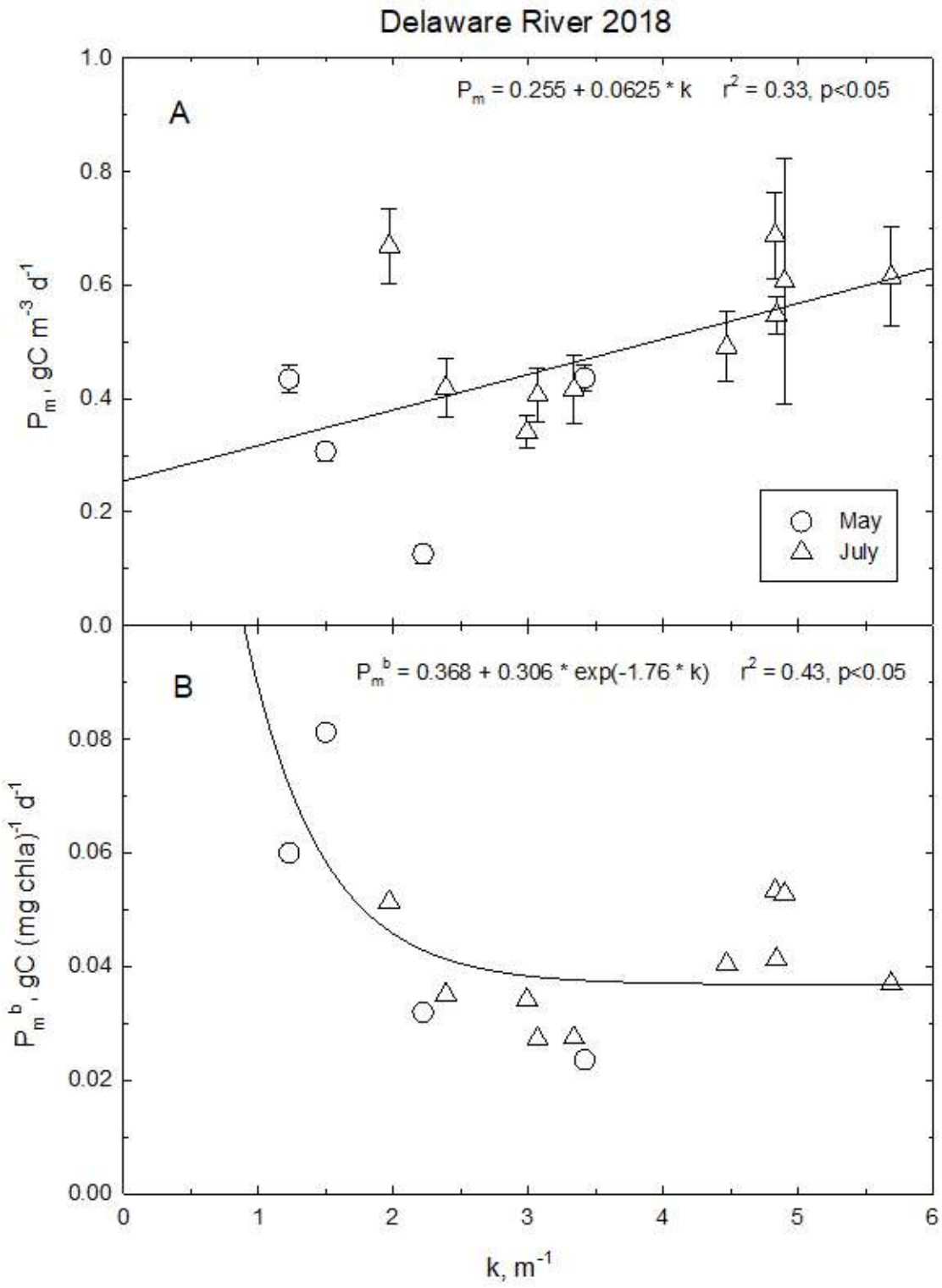

Figure 9B. The relationship of the light-saturated photosynthetic parameters P_m and P_m^b to the water column extinction coefficient for PAR (k). There was a significant, linear relationship between Pm and k (upper panel), and a significant, inverse exponential relationship between P_m^b and k (lower panel) in the combined dataset.

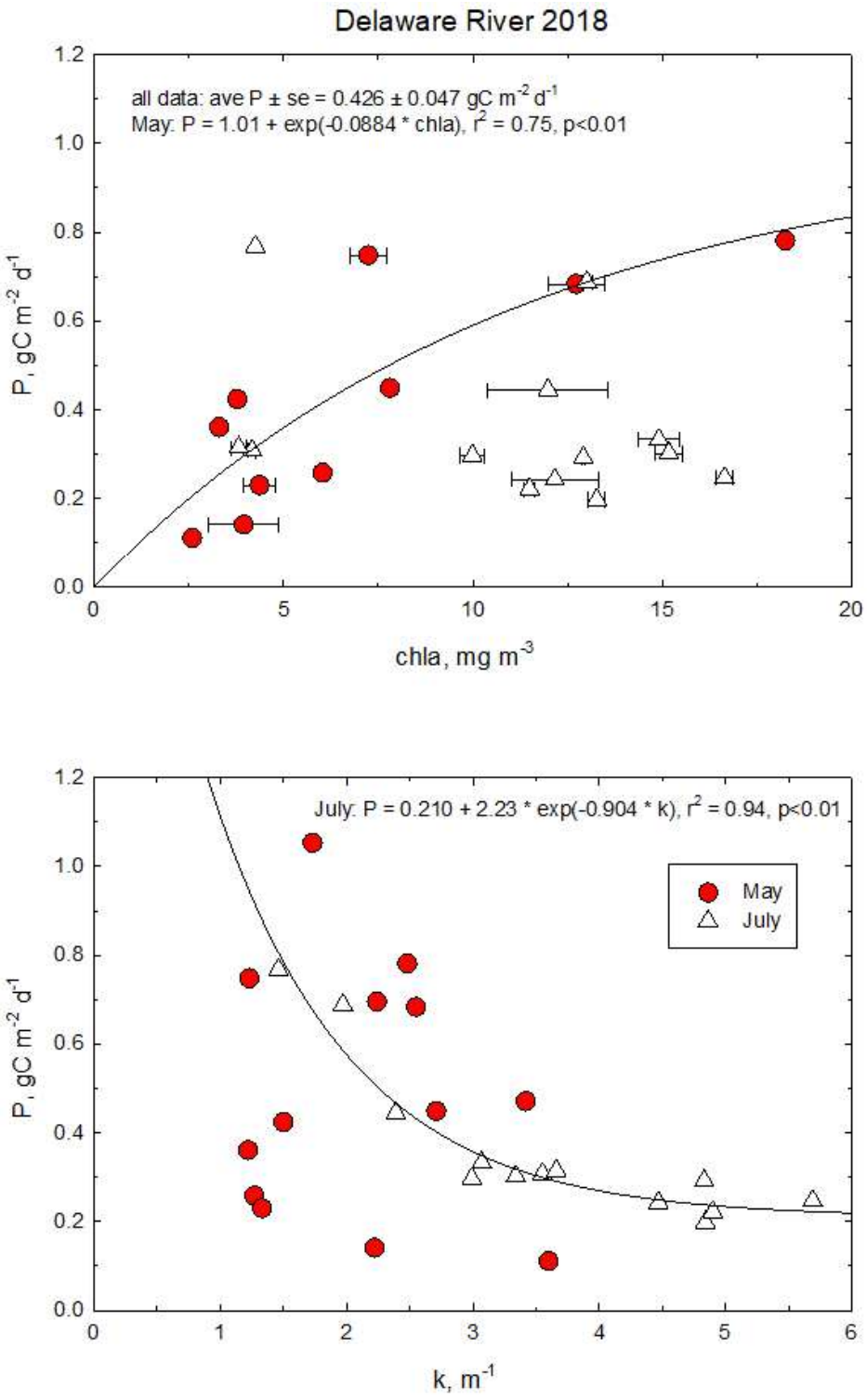

Figure 10. Primary productivity (P) in the water column as a function of surface chlorophyll *a* for May but not July 2018 (upper panel), and the relationship of P to the water column extinction coefficient for July, but not for May (lower panel). Compression of the lighted (euphotic) zone by high k is evident in these data, limiting water column integrated production (P).